

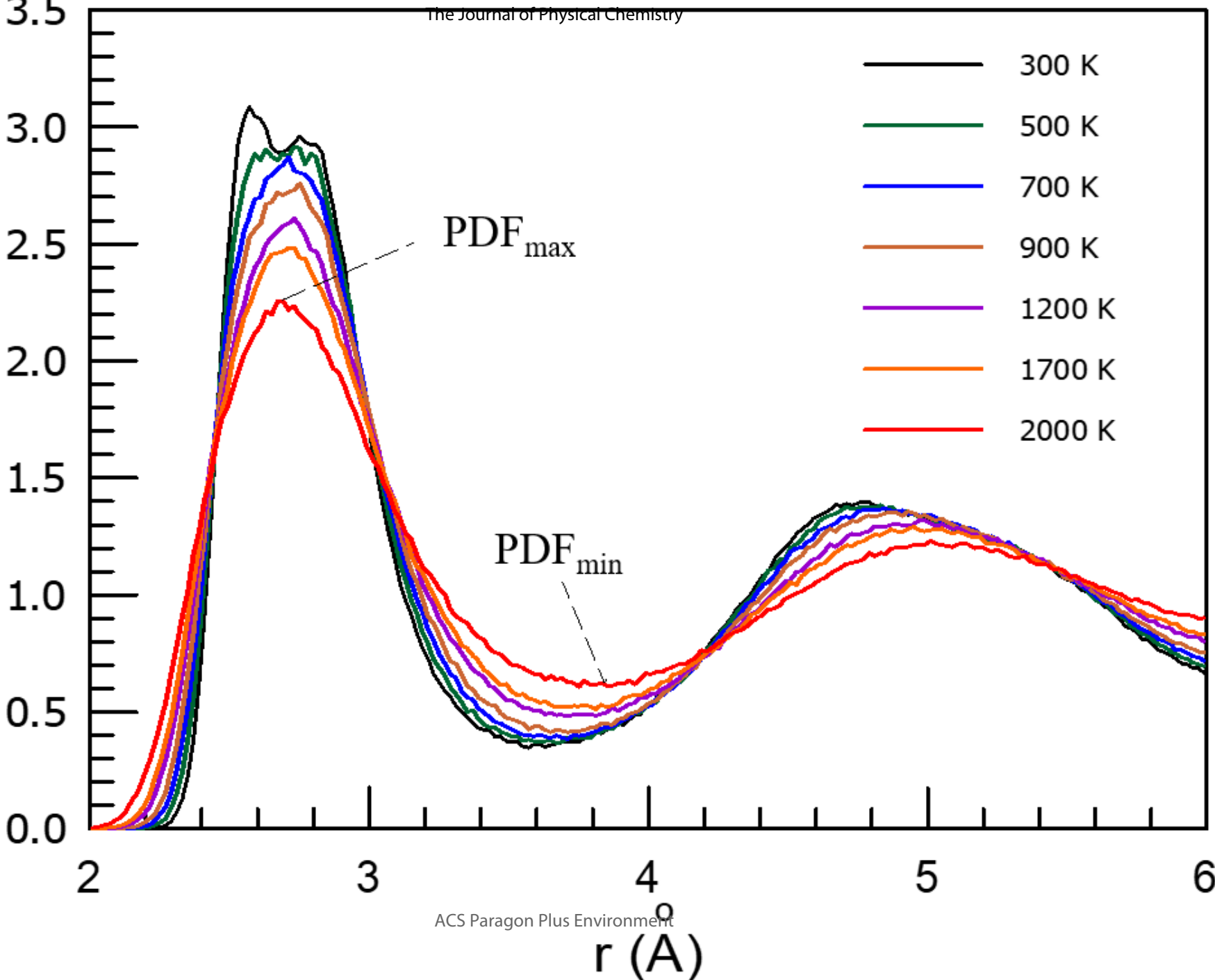
This document is confidential and is proprietary to the American Chemical Society and its authors. Do not copy or disclose without written permission. If you have received this item in error, notify the sender and delete all copies.

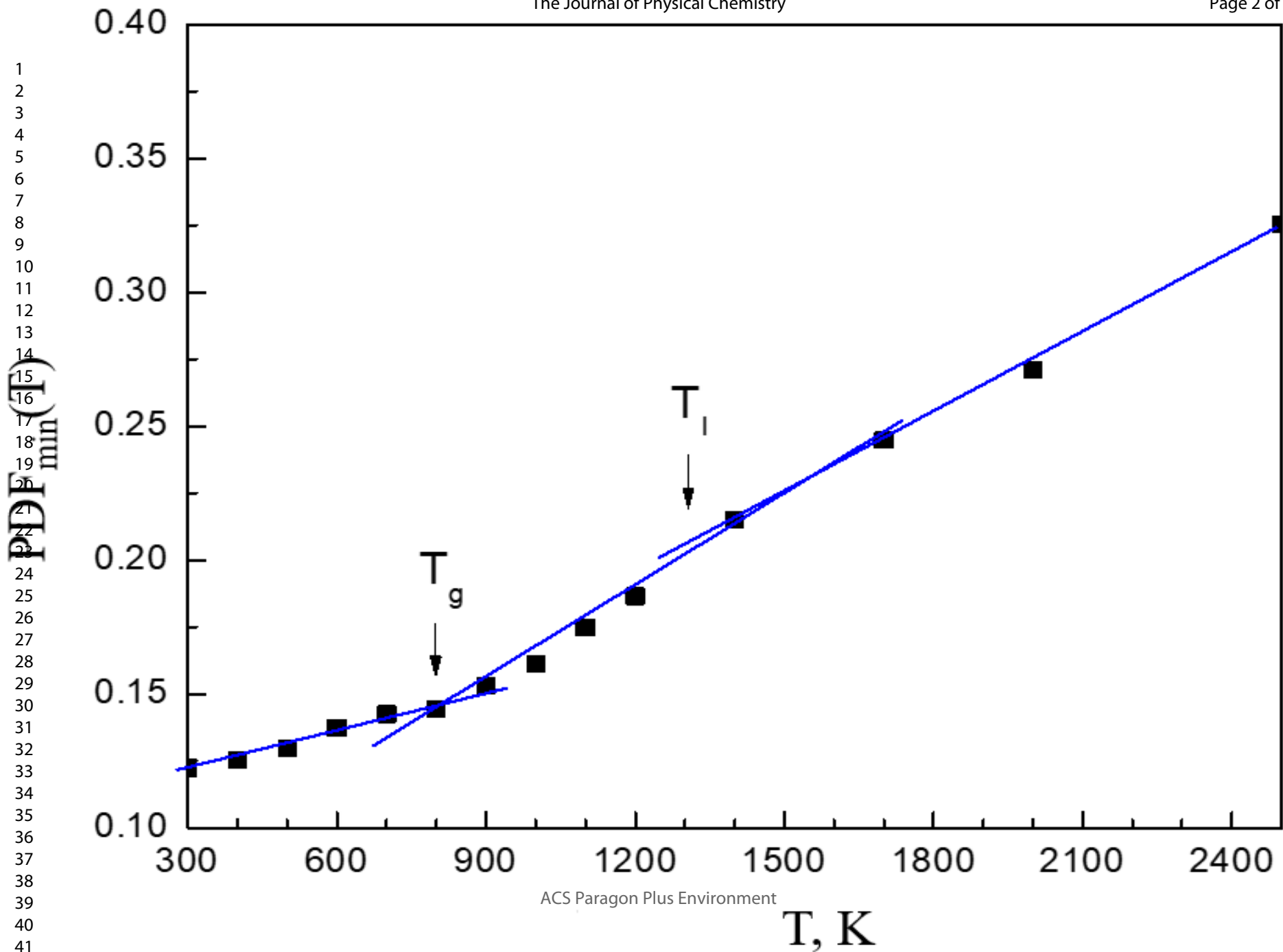
Revealing Structural Changes at Glass Transition via Radial Distribution Functions

Journal:	<i>The Journal of Physical Chemistry</i>
Manuscript ID	jp-2020-00214b.R2
Manuscript Type:	Article
Date Submitted by the Author:	n/a
Complete List of Authors:	Ojovan, Michael; Imperial College London, Department of Materials Louzguine-Luzgin, Dmitri; Tohoku University, WPI Advanced Institute for Materials Research

SCHOLARONE™
Manuscripts

1
2
3
4
5
6
7
8
9
10
11
12
13
14
15
16
17
18
19
20
21
22
23
24
25
26
27
28
29
30
31
32
33
34
35
36
37
38
39
40
41





1
2
3
4
5
6
7
8
9
10
11
12
13
14
15
16
17
18
19
20
21
22
23
24
25
26
27
28
29
30
31
32
33
34
35
36
37
38
39
40
41

Atomic volume, Å³/at.

— 128000 at. at 10¹² K/s
— 128000 at. at 10¹³ K/s

Glass
T_g
Super-cooled liquid
T_l ~ 1273 K
Liquid

15.0

500

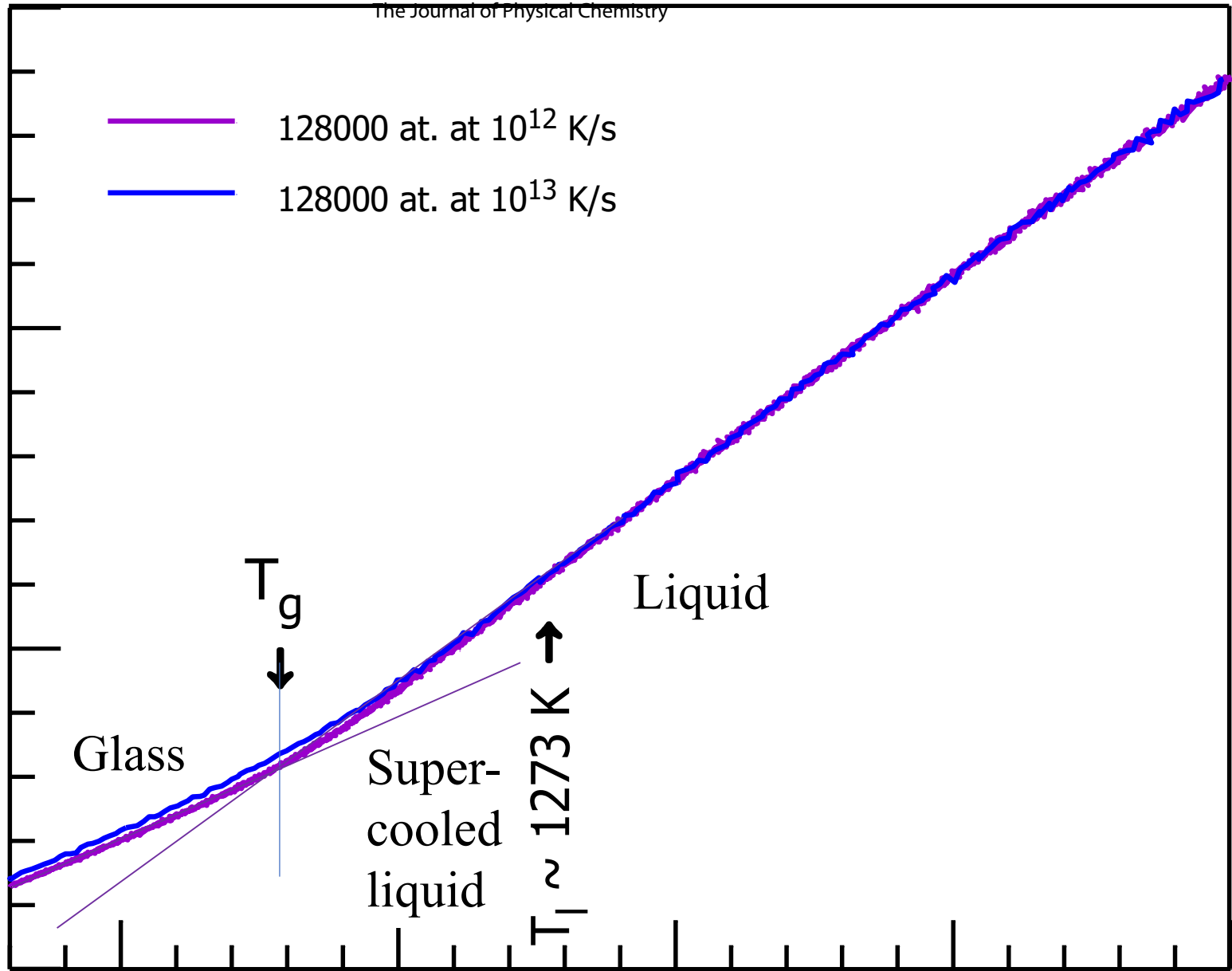
1000

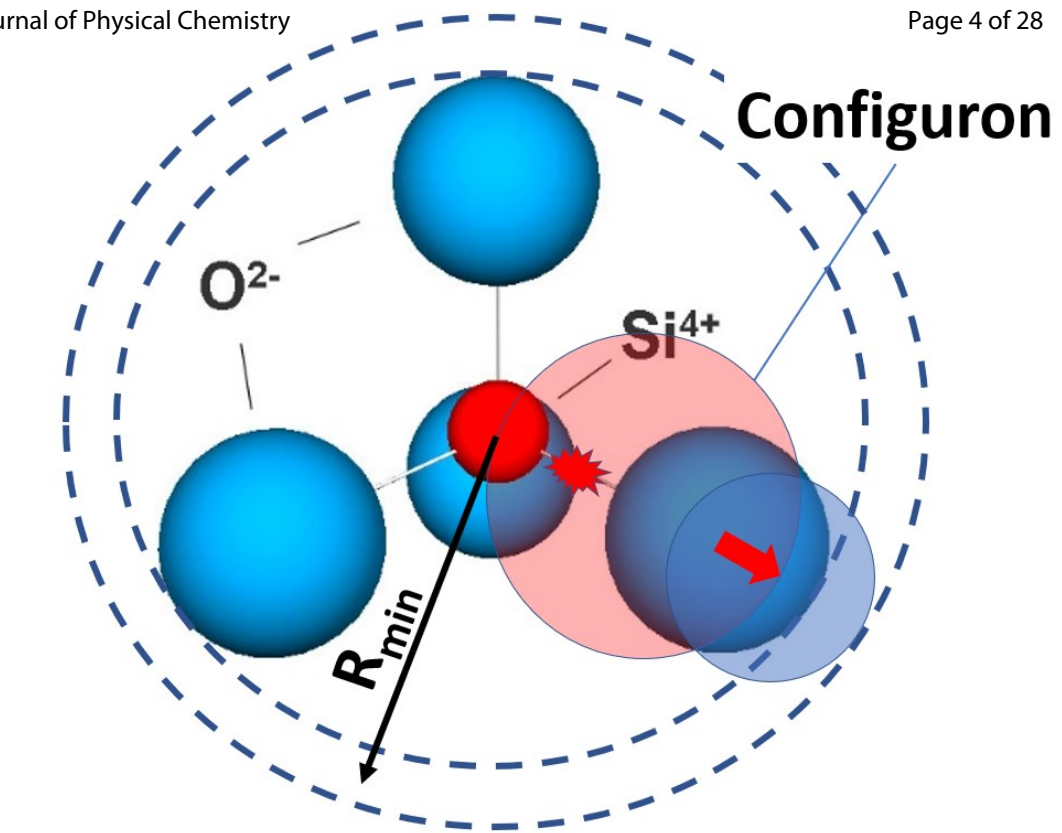
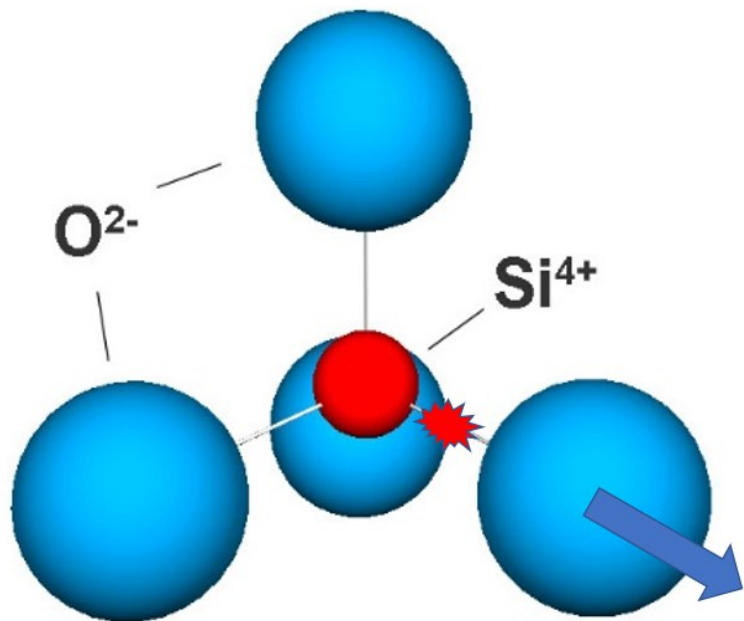
1500

2000

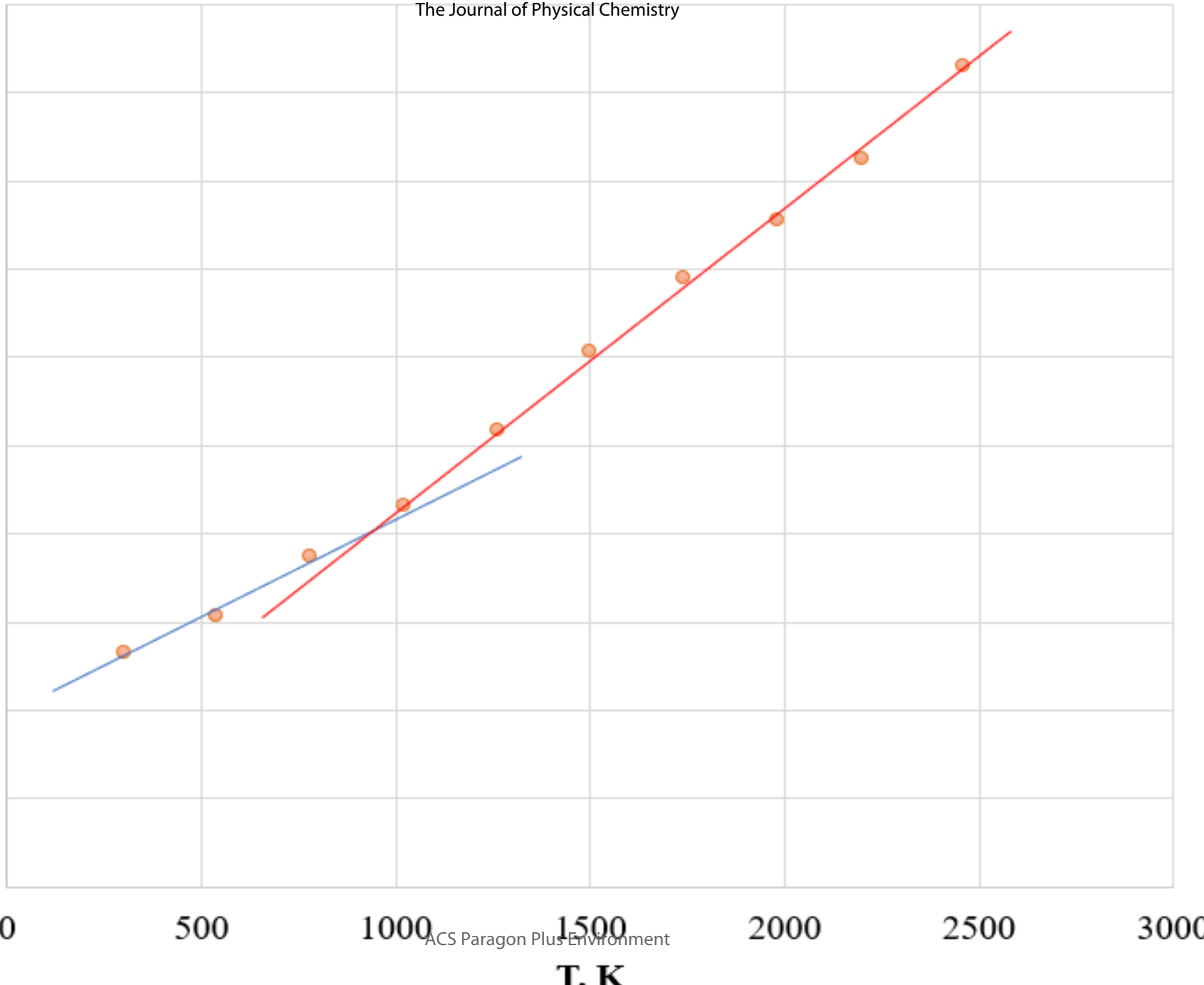
2500

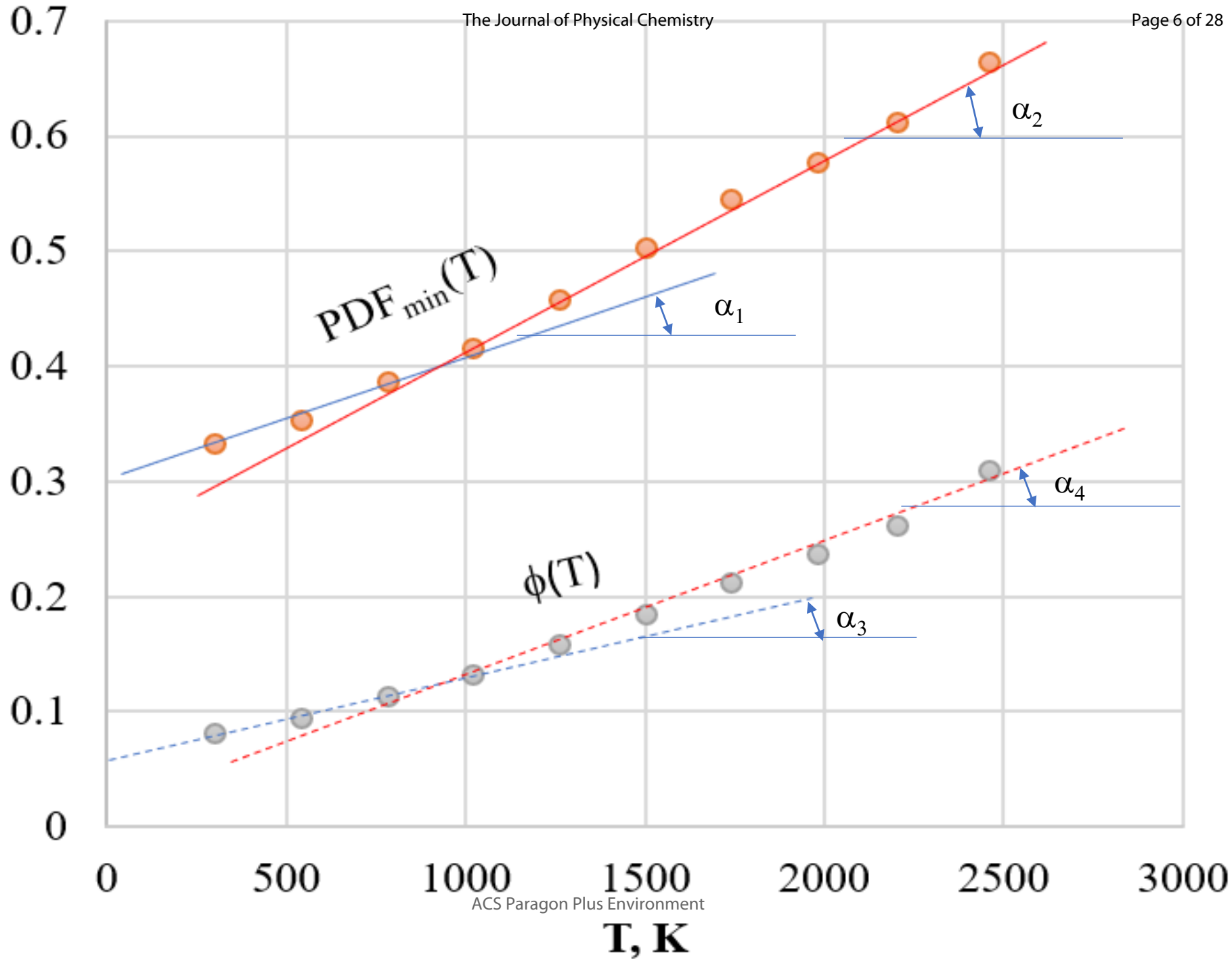
T, K



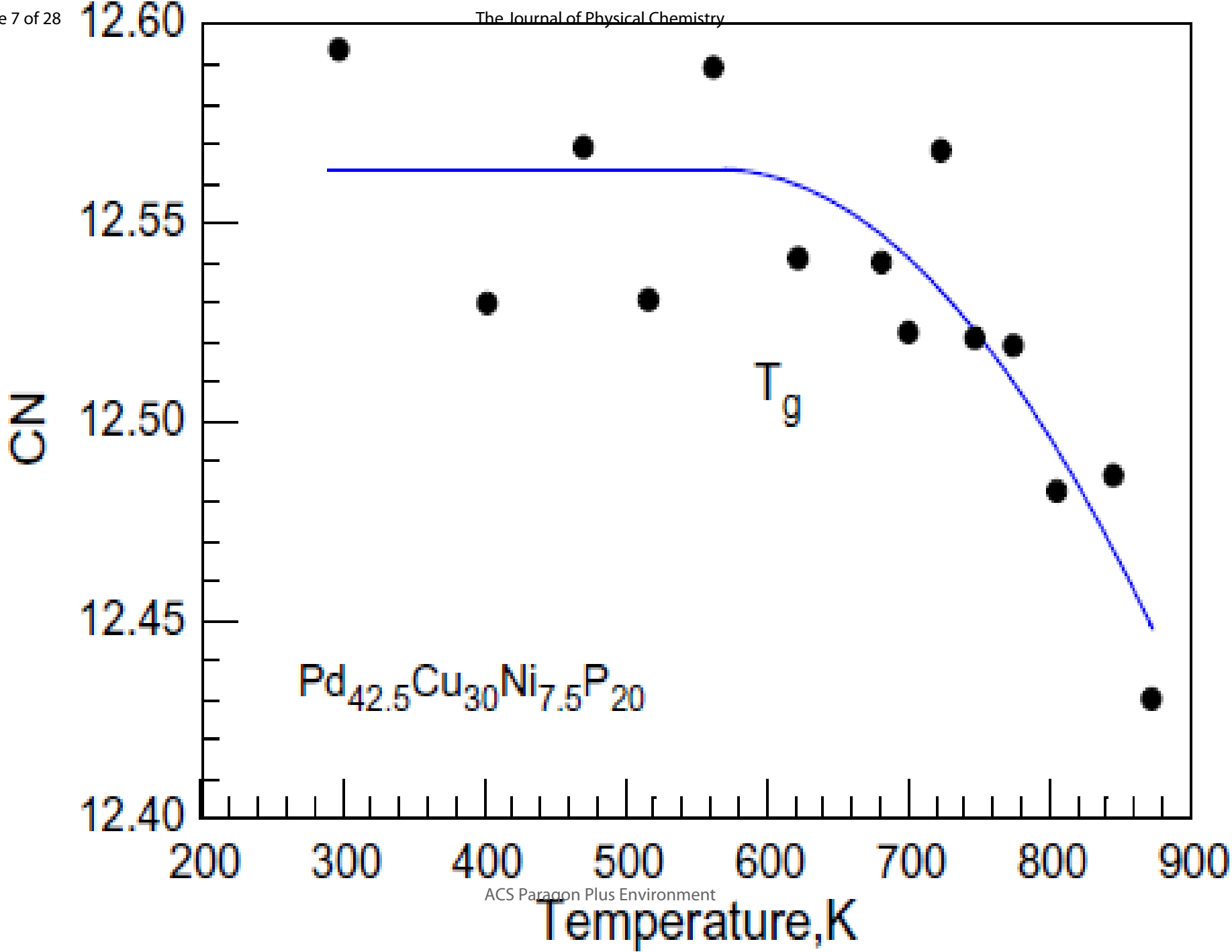


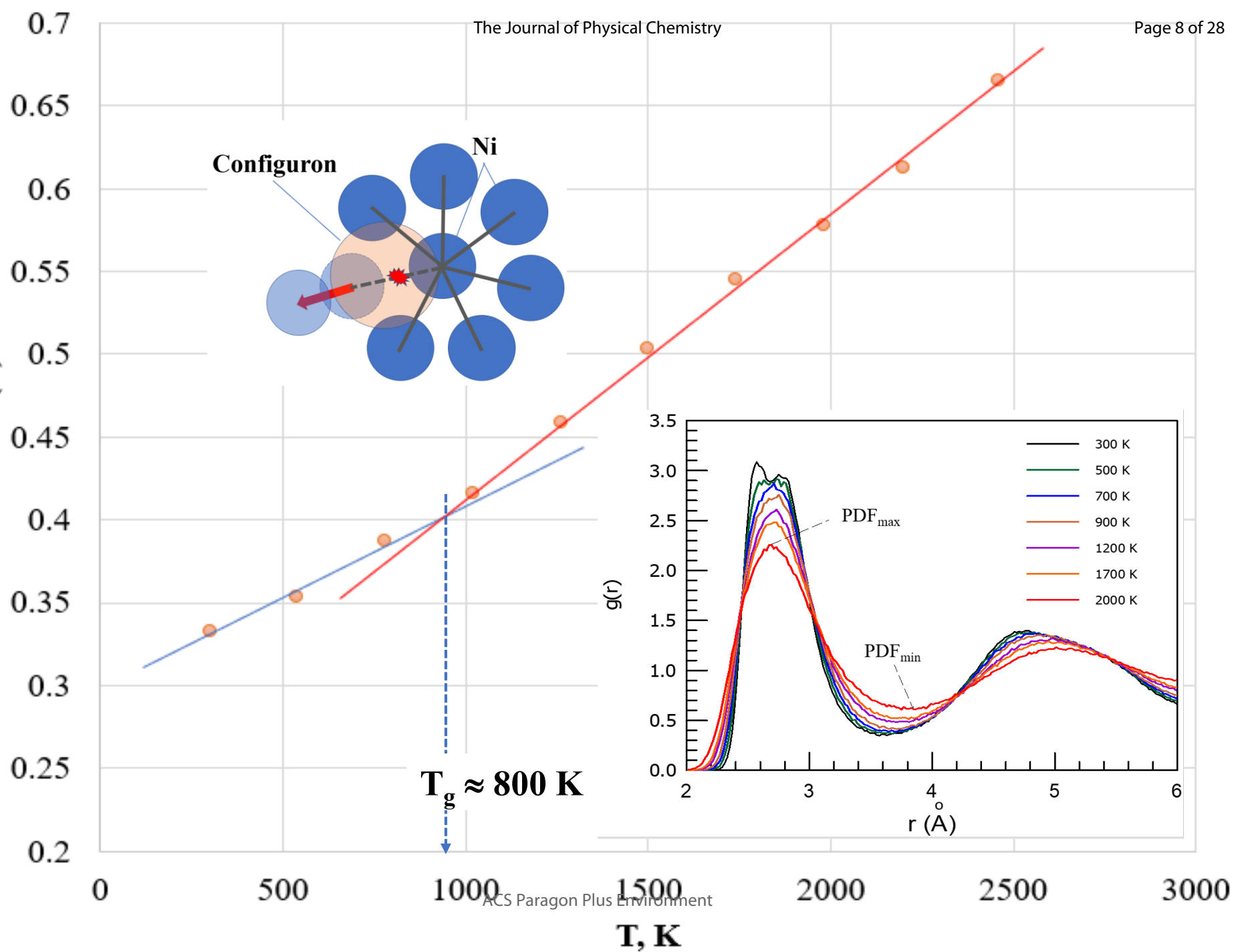
1
2
3
4
5
6
7
8
9
10
11
12
13
14
15
16
17
18
19
20
21
22
23
24
25
26
27
28
29
30
31
32
33
34
35
36
37
38
39
40
41



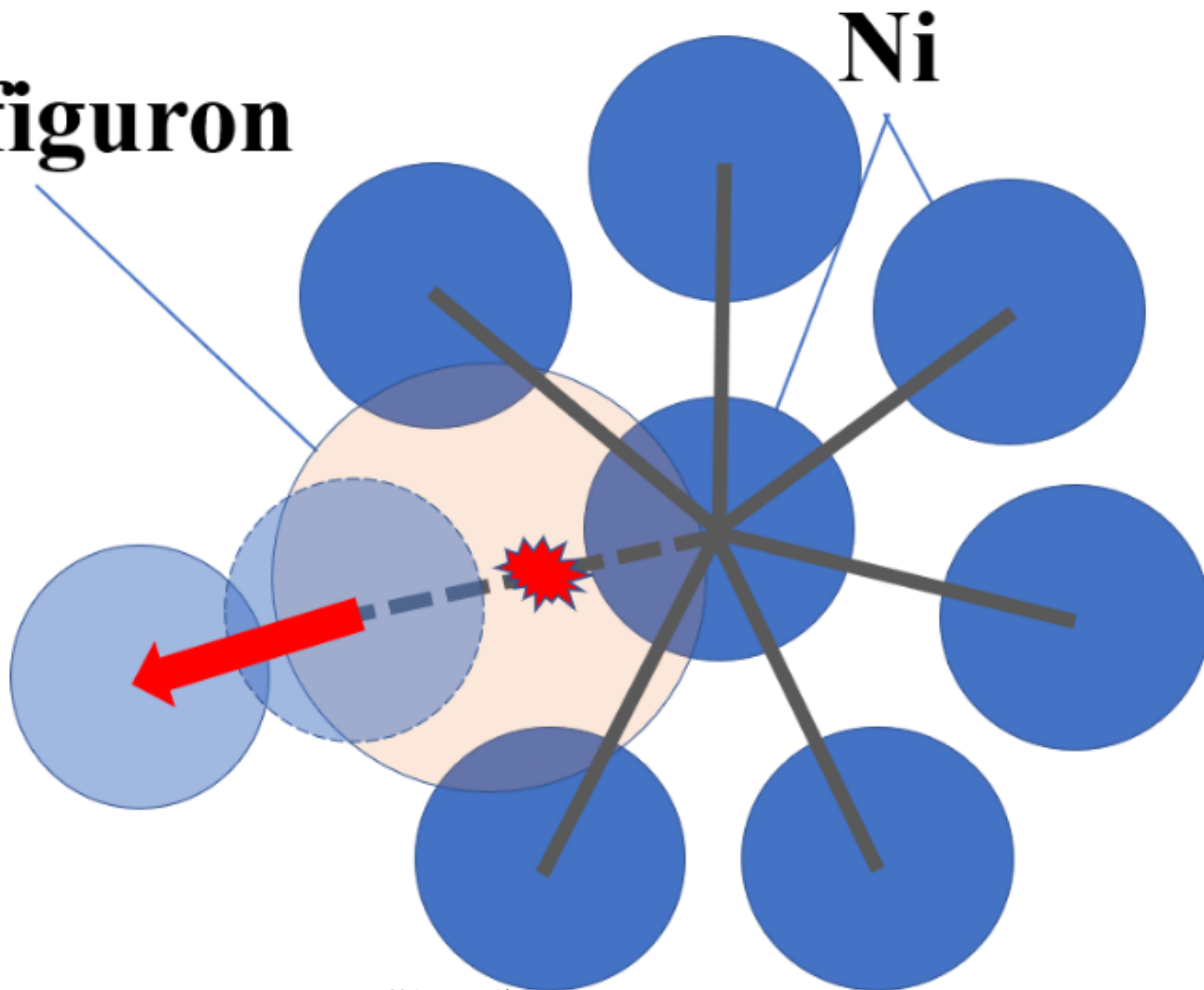
1
2
3
4
5
6
7
8
9
10
11
12
13
14
15
16
17
18
19
20
21
22
23
24
25
26
27
28
29
30
31
32
33
34
35
36
37
38
39
40
41

1
2
3
4
5
6
7
8
9
10
11
12
13
14
15
16
17
18
19
20
21
22
23
24
25
26
27
28
29
30
31
32
33
34
35
36
37
38
39
40
41



1
2
3
4
5
6
7
8
9
10
11
12
13
14
15
16
17
18
19
20
21
22
23
24
25
26
27
28
29
30
31
32
33
34
35
36
37
38
39
40
41

Configuron



Revealing Structural Changes at Glass Transition via Radial Distribution Functions

Michael I. Ojovan^{1,2*}, Dmitri V. Louzguine-Luzgin^{3,4}

¹Department of Materials, Imperial College London, South Kensington Campus, Exhibition Road, London SW7 2AZ, United Kingdom

²Institute of Geology of Ore Deposits, Petrography, Mineralogy and Geochemistry (IGEM), Russian Academy of Sciences, Russia

³WPI Advanced Institute for Materials Research, Tohoku University, Aoba-Ku, Sendai 980-8577, Japan

⁴MathAM-OIL, National Institute of Advanced Industrial Science and Technology (AIST), Sendai 980-8577, Japan

Abstract

Transformation of glasses into liquids is discussed in terms of configuron (broken chemical bond or transformation of an atom from one to another atomic shell) percolation theory with structural changes caused. The first sharp diffraction minimum (FSDM) in the pair distribution function (PDF) is shown to contain information on structural changes in amorphous materials at the glass transition temperature (T_g). A method to determine the glass transition temperature is proposed based on allocating T_g to the temperature when a sharp kink in FSDM occurs. The method proposed is more sensitive compared with empirical criterion of Wendt-Abraham e.g. for amorphous Ni the kink that determines T_g is almost twice sharper. Connection between the kink in fictive temperature behaviour of PDF and Wendt-Abraham criterion is discussed.

Introduction

Transformation of a liquid on cooling into a glass (i.e. glass transition) can take place at melt cooling rates rapid enough that crystallisation is kinetically avoided. Glass transition phenomena are observed universally moreover all liquids can be in practice vitrified provided that the rate of cooling is high enough to avoid crystallisation. The difficulty to understand the glass transition is because of almost undetectable changes in the structure of amorphous materials despite of the qualitative changes in characteristics and extremely large change in the time scale of relaxation processes. Because of that the glass transition is still debated whether is really a phase transformation or just a gradual although considerable change of material viscosity the result of which being the delayed mechanical relaxation to longer that observation times¹⁻⁴.

Generically glasses are solid amorphous materials which on temperature increase above a certain temperature termed glass transition temperature (T_g) transform into liquids that are typically amorphous (apart from liquid crystals). On cooling melts vitrify at T_g e.g. transform into glasses if they bypass crystallisation which in many cases occurs if the cooling rate is not enough fast. Arbitrarily the glass-transition temperature is defined as a temperature at which the equilibrium viscosity of the melt reaches 10^{12} Pa·s. However, it can be well measured on

1
2
3 cooling only for such good glass-formers as SiO₂ while many other substances will
4 crystallize upon measurement on cooling.
5

6 The glass transition is experimentally observed as a second-order phase transformation in the
7 Ehrenfest sense with continuity of material volume and entropy, and discontinuity of their
8 derivatives which are therefore used in practice to detect where transformation occurs e.g. to
9 detect the T_g^{4,5}. Moreover, the International Union of Pure and Applied Chemistry (IUPAC)
10 defines glass transition as a second-order transition in which a supercooled melt yields, on
11 cooling, a glassy structure” so that “below the glass-transition temperature the physical
12 properties vary in a manner similar to those of the crystalline phase⁶. Glass transition is often
13 considered as a true phase transformation that belongs to critical phenomena generically
14 termed topological phase transitions which are amenable to the scaling approach and
15 characterised by diverging length and time at the transition^{2, 7-9}. E. g. configuron percolation
16 theory treats glass-liquid transition as the case of percolation via broken bonds (e.g.
17 configurons)^{10, 11}. There are several descriptions of glass transition as a true phase
18 transformation. A typical model is based on a percolation-type phase transition with the
19 formation of dynamic fractal structures close to the percolation threshold¹². Macroscopic
20 percolating clusters formed at the glass transition have been visualized¹³. High precision
21 measurements of fifth-order, non-linear dielectric susceptibilities of growing transient
22 domains diverge towards T_g¹⁴. Excited delocalized atoms would be responsible for
23 facilitating viscous flow and explaining time dependence of T_g. At the glass transition, the
24 process of atom delocalization would be reduced without being fully eliminated¹⁵.

25 Theoretical works based on the notion that a random first-order transition lies at the heart of
26 glass formation have been also developed. The possible existence of an underlying first-order
27 transition without latent heat has been raised¹⁶⁻¹⁹. Its role in many glass-forming melts has
28 been explicitly shown³ e.g. Tournier considers the transition at T_g as due to a change of the
29 undercooled-liquid Gibbs free energy, which is the driving force of the glass transition. In
30 this approach the classical Gibbs free energy change for a crystal formation has been
31 modified to account for the enthalpy saving which allowed decent description of liquid-liquid
32 and stable glass transitions^{20, 21}. Direct structural changes upon glass transition have been
33 revealed by *in-situ* studies of glass transition by synchrotron XRD via reciprocal and real-
34 space radial distribution functions²²⁻²⁴.

35 The crucial difficulty in accepting or rejecting the concept of phase transition in amorphous
36 materials is related to the absence of readily detectable structural changes at glass transition.
37 In contrast to crystallisation leading to obvious symmetry changes and formation of a
38 periodic anisotropic structure vitrification maintains the same topological disordered structure
39 making almost impossible to distinguish structurally a glass from a melt. Here we emphasise
40 the possibility of utilising data from neutron or X-ray diffractometry to reveal those almost
41 undetectable changes in the structure of amorphous materials at glass transition based on
42 physical meaning of parameters obtained and using the concept of broken chemical bonds
43 (configurons). As the percolation model of glass-liquid transition treats transformation of
44 glasses into liquids at glass transition as an effect resulting from percolation via broken bonds
45 (e.g. configurons) we first briefly analyse this model.
46
47
48
49
50
51
52
53

54 **Configuron percolation model of glass-liquid transition**

55 The difficulty in describing a system of strongly interacting atoms in a condensed state such
56 as an amorphous material either liquid or solid can be facilitated by using bond lattice model
57 which was proposed by Angel and Rao aiming to replace the set of atoms by a congruent
58 structure of weakly interacting bonds – the congruent bond lattice (CBL)²⁵. In the CBL the
59
60

1
2
3 system of weakly-interacting chemical bonds denoted as •, congruently replaces the initial
4 system of strongly interacting cations such as Si⁺⁴ and O⁻² in SiO₂. Thus, the system of N
5 strongly interacting cations (Si⁺⁴ for silica glass) and anions (O⁻² for silica glass) is replaced
6 by a system of N'=NZ weakly interacting bonds where Z is the coordination number (Z=4 for
7 silica glass). In the case when atoms are not bonded via bridging atoms (like oxygen in
8 silica), which is typical for metallic glasses for example for glassy Ni, then N'=NZ/2.

9
10 Temperature fluctuations break some of bonds so that on increase of temperature more and
11 more bonds are broken until percolation via broken bonds occurs which results in a kind of
12 disintegration or transformation of a solid to a liquid²⁶. Hence the possibility to detect the
13 transformation of a glass into a liquid e.g. glass transition appears based on CBL. Moreover,
14 the system of bonds e.g. the CBL looks very much like a system of contacting although
15 practically not interacting. Spheres packed in a disordered arrangement create a contact
16 network with the number of neighbours of each node in this network between four and twelve
17 with an average of six²⁷. A natural question to that system is on what percolation threshold of
18 this network is²⁸. E.g. if a certain fraction p of spheres is conducting and the rest are non-
19 conducting then what is the value of critical fraction p_c at which long-range conduction first
20 occurs? Conducting spheres in our case are equivalent to broken bonds whereas non-broken
21 bonds are equivalent to non-conducting spheres. Also, in analysis we assume that the radii of
22 broken bonds in first approximation are equal to radii of unbroken bonds although account
23 should be paid on increase of radii on bond breakage. An important development in the
24 understanding of percolation thresholds in disordered (randomly distributed) systems was the
25 introduction of the critical volume fraction (θ_c) by Scher and Zallen²⁹. For regular lattices of
26 any objects such as spheres with uniform nearest-neighbour bond lengths of unity, they
27 considered placing spheres of unit diameter at each vertex with fraction of space occupied by
28 spheres giving the filling fraction f. Multiplying this quantity by the site percolation threshold
29 p_c yields θ_c = p_cf. For the three-dimensional systems that were studied, it was found that the
30 θ_c falls in a narrow range of 0.144 – 0.163 e.g. generically the invariant occurs for the critical
31 volume fraction θ_c = 0.15 ± 0.01. This fraction is often termed Sher-Zallen invariant²⁸.
32 Important to note that in contrast to free-volume model of liquid-glass transition³⁰ the
33 configuron percolation model operates with the volume of configurons which is related to
34 chemical bonds only and not to the free (e.g. non-occupied) volume⁷⁻¹².

35
36 Bond breaking process that leads to formation of configurons can be represented as a reaction
37 when a lattice excitation (phonon) is absorbed by a bond (designation ·) resulting initially in a
38 un-relaxed broken bond which after relaxation of the surrounding environment results in the
39 formation of a quasiparticle termed configuron (designation o):



41
42 Melting of an amorphous material occurs when broken bonds form a percolation cluster that
43 changes macroscopically the rigidity of system. Using this concept, we can analytically
44 calculate the concentration of broken bonds, that can be readily done at least for simply
45 systems^{7,8}. Indeed, below and approaching glass-liquid transition temperature T_g the
46 concentration of configurons can be calculated as a function of temperature using an
47 equivalent simple two-level system that consists of unbroken (ground level) and broken
48 (excited level) bonds⁷⁻¹². That gives the explicit equation of configuron concentration C_d:

$$49 \quad C_d = C_0 \frac{\exp(-G_d/RT)}{1 + \exp(-G_d/RT)} \quad (2)$$

50
51 where G_d is the configuron formation Gibbs free energy G_d = H_d - TS_d, H_d is the enthalpy
52 and S_d is the entropy of formation of configurons.
53
54
55
56
57
58
59
60

Designate the fraction of broken bonds as $\phi(T)=C_d/C_0$. The condition when fraction of broken bonds $\phi(T)$ equalises the percolation threshold $\phi_c = \theta_c = 0.15 \pm 0.01$ determines when the first time a percolation cluster made of broken bonds – configurons – is formed. It thus gives the temperature of glass transition of an amorphous materials which is directly related to the enthalpy H_d and entropy S_d of configurons – broken bonds:

$$T_g = \frac{H_d}{S_d + R \ln[(1 - \phi_c)/\phi_c]} \quad (3)$$

T_g is hence dependent on quasi-equilibrium thermodynamic parameters of bonds e.g. on enthalpy (H_d) and entropy (S_d) of formation of bonds (configurons) at given conditions (not necessarily equilibrium).

The glass-liquid transition in the configuron percolation model shows typical features of second order phase transformations so that derivatives parameters such as thermal expansion coefficient and specific heat capacity diverge at T_g . Namely, the heat capacity of glasses C_p near T_g (at scan up of temperature) behaves as $C_p \sim |T_g - T|^{-0.59}$ due to formation of percolation cluster made of configurons^{7,8}.

Interestingly that melts vitrification is not accompanied by configuron clusters formation, thus on glass formation from melts there should not be associated discontinuities in temperature dependence of C_p , e.g. on scan down of temperature. Moreover, the configurons are present only as point defects and small clusters made of such defects in glasses, e.g. the configuron percolation model naturally explains the experimentally seen hysteresis in the behaviour of heat capacity near glass transition at both scan up and scan down of temperatures neat T_g .

The fraction $\phi(T)$ of broken bonds decreases during cooling down to 0.15 and below. However, as noted by Tournier³¹, this cannot occur after reheating the glassy phase because $\phi(T)$ could remain equal to 0.15 up to the higher temperatures where the coherence length becomes small e.g. equal to mean interatomic distance. We note in this respect the work of Wei and et.al.³² which has reported on a detected first-order transition in the melt at the temperature where the event occurs at the predicted temperature T_n ³.

The configuron percolation model envisages that structurally melts have a fractal geometry of bonds with broken bonds forming extended (macroscopic) fractals and because of that a liquid-like behaviour, and glasses have a 3-D geometry of bonds with point-type broken bonds having a 0-D geometry and because of that a solid-like behaviour.

Configurons and clusters made of configurons cannot be directly observed as these are excitations of CBL. We suggest herewith detection of direct results of configuron formation – namely of atomic displacements caused by configuron and clusters of configuron formation.

The PDF's approach to structural changes

A powerful method to investigate the structure of liquids and glasses is utilising scattering of incident neutron or X-rays by the sample and detection of all scattered quanta e.g. neutron and X-ray diffraction techniques^{33, 34}. The scattered radiation amplitude $A(\mathbf{q})$ from an array of N point atoms at positions $\mathbf{R}_1 \cdots \mathbf{R}_N$ is given by $A(\mathbf{q}) = \sum_j b_j \exp(i\mathbf{q} \cdot \mathbf{r}_j)$, where b_j is the scattering length (form factor) for atom j ³⁴. The scattered intensity of x-rays per unit atom $I(\mathbf{q}) = \frac{1}{N} \sum_{jk} b_j b_k \exp(i\mathbf{q} \cdot (\mathbf{r}_j - \mathbf{r}_k))$, which is expressed for anisotropic materials like glasses and melts in terms of structural factor $S(\mathbf{q})$. The structure of a monatomic isotropic sample can be described in real space in terms of its pair-distribution function (PDF) $g(r)$ -PDF(R)

which is proportional to the probability of finding an atom at a position $r = R$ relative to a reference atom taken to be at the origin. The PDF is related to static structure factor $S(q)$ via

$$g(r) = 1 + \frac{1}{2\pi^2 r \rho_0} \int_0^\infty q [S(q) - 1] \sin(qr) dq \quad (4)$$

where ρ_0 is the density, q is the scattering vector which for a quantum of incident wavelength λ_0 is related to the scattering angle 2θ via relation

$$q = \frac{4\pi}{\lambda_0} \sin\theta \quad (5)$$

As liquid and glasses are overall isotropic structures the diffraction pattern has conical symmetry and the azimuthal angle ϕ of the scattered quanta is not specified. That reduces the 3D analytical approach to an effective 2D system with two variables e.g. r and θ .

By construction, $g(r)$ is dimensionless, moreover $S(q \rightarrow \infty) = 1$ and $g(r \rightarrow \infty) = 1$. The average number n_{av} of neighbouring atoms in a coordination shell located between r_1 to r_2 is given by:

$$n_{av} = 4\pi\rho_0 \int_{r_1}^{r_2} g(r) r^2 dr \quad (6)$$

E.g. r_1 and r_2 can be distances corresponding to consecutive minima in $g(r)$. The average number of atoms in the first such shell is termed the coordination number (CN).

Anisotropy in amorphous materials can be induced by stresses therefore for anisotropic systems anisotropic PDF method should be used which is based on the expansion by spherical harmonics³⁵. Also, if there is more than one atom type (oxygen, sodium, etc.) present then the PDF is typically split into several terms, one for each pair of atomic species³⁶. The $g_{\alpha\beta}(r)$ would be the pair correlation function between atoms of type α and β which can be used to calculate respective coordination numbers e.g. the number of β -type atoms around an α -type atom at the origin:

$$N_{\alpha\beta} = 4\pi\rho_\beta \int_{r_1}^{r_2} g_{\alpha\beta}(r) r^2 dr \quad (7)$$

The forms of PDF's $g(r)$ or $g_{\alpha\beta}(r)$ which are proportional to the probability of finding an atom at a position r relative to a reference atom can be used to understand changes that occur in glasses and melts on temperature variations including structural modifications at glass transition. Indeed, the maxima of $g(r)$ are positioned at most probable radii where atoms reside whereas minima are related to bond distances. Thus, the first peak of PDF_{max} , that is often termed first sharp diffraction peak (FSDP)³⁷⁻³⁹, corresponds to atoms in the first coordination shell e.g. coordinated with the given atom, whereas the first sharp diffraction minimum (FSDM) is positioned at the end of first coordination shell and corresponds to bonds connecting atoms. This were illustrated by data for H_2O that produces a negative peak at the OH bond distance³⁴. The following peaks of $PDF(R)$ correspond to next coordination shells. At large distances $r = R \rightarrow \infty$ the limit holds $PDF(R) \rightarrow 1$. Fig. 1 demonstrates typical $PDF(R) = g(r)$ behaviour of amorphous Ti_2Ni alloy obtained via molecular dynamic (MD) simulations with R_{max} corresponding to FSDP whereas R_{min} to FSDM of PDF.

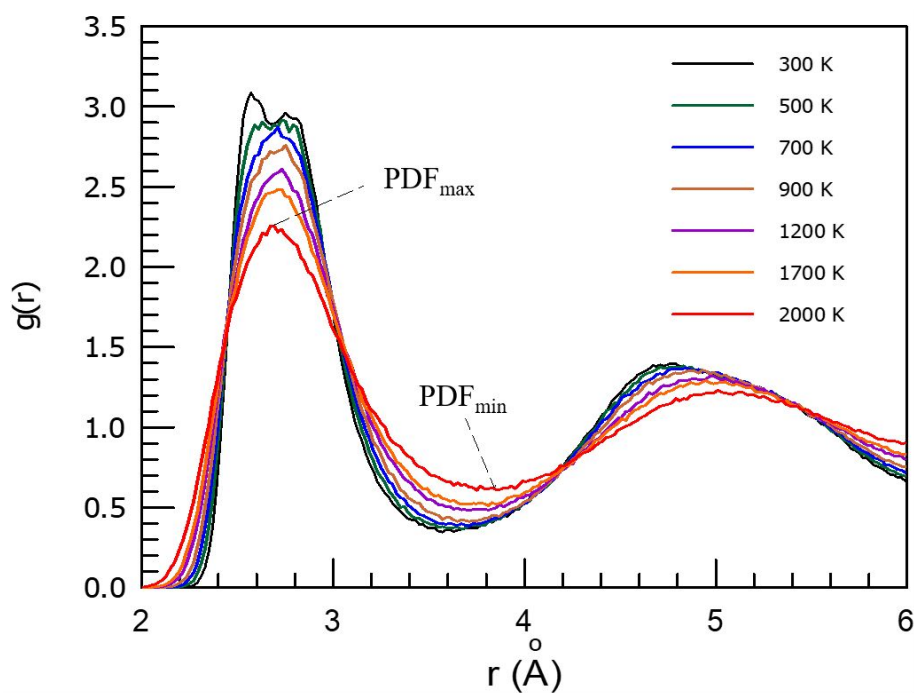


Fig. 1. Pair-distribution function $PDF(R) = g(r)$ of amorphous Ti_2Ni ($Ti_{67}Ni_{33}$) alloy obtained via molecular dynamic (MD) simulations at cooling rate 10^{12} K/s.

To model glass-formation of $Ti_{67}Ni_{33}$ metallic glass MD computer simulation was applied using the software package LAMMPS for classical molecular dynamics^{40, 41}. Simple cubic crystalline cells containing 16000 and 128000 atoms were treated by heating the cell from 300 to 3000 K, holding at 3000 K for 30 ps, cooling down to 300 K at different cooling rates. The Embedded-Atom Method (EAM) potential for the Ti-Ni system was used from Ref.⁴². The simulation was carried out with 1 fs time steps under NPT (constant atom number, pressure and temperature) and periodic boundary conditions. The Nose-Hoover thermostat^{43, 44} and a barostat⁴⁵ were used to control the temperature and pressure, respectively. A software package “OVITO”⁴⁶ was used to visualize and analyse simulation results. Glass-formation process of Ti_2Ni alloy was modelled at the cooling rates ranging from 10^{11} K/s to 10^{13} K/s. Fig. 1 above showed $PDF(r)$ of the sample cooled at 10^{12} K/s. Fig. 2 indicates the value of PDF_{min} after the maximum corresponding to the first coordination shell.

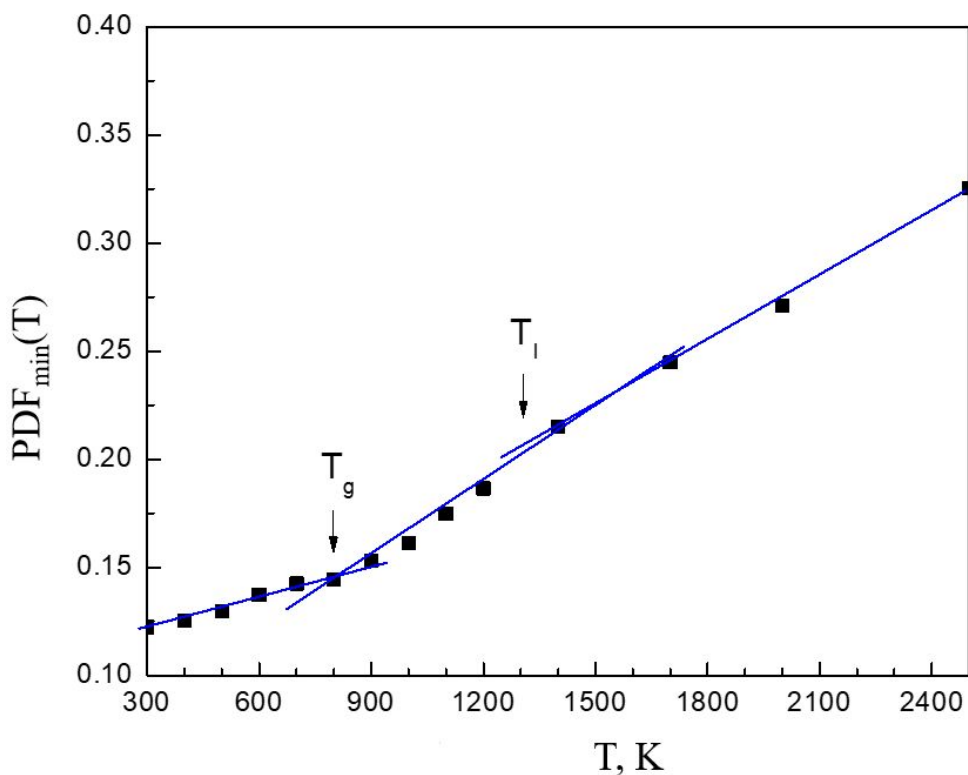


Fig. 2. The first sharp diffraction minimum (FSDM) value of PDF after the first sharp diffraction peak (FSDP) of amorphous Ti_2Ni corresponding to the first coordination shell as shown in Fig. 1. T_g indicates the glass transition temperature and T_l the liquidus temperature. There is another change of slope slightly above T_l which may indicate other structural changes in the equilibrium liquid.

Fig. 3 indicates the atomic volume of amorphous Ti_2Ni as a function of temperature.

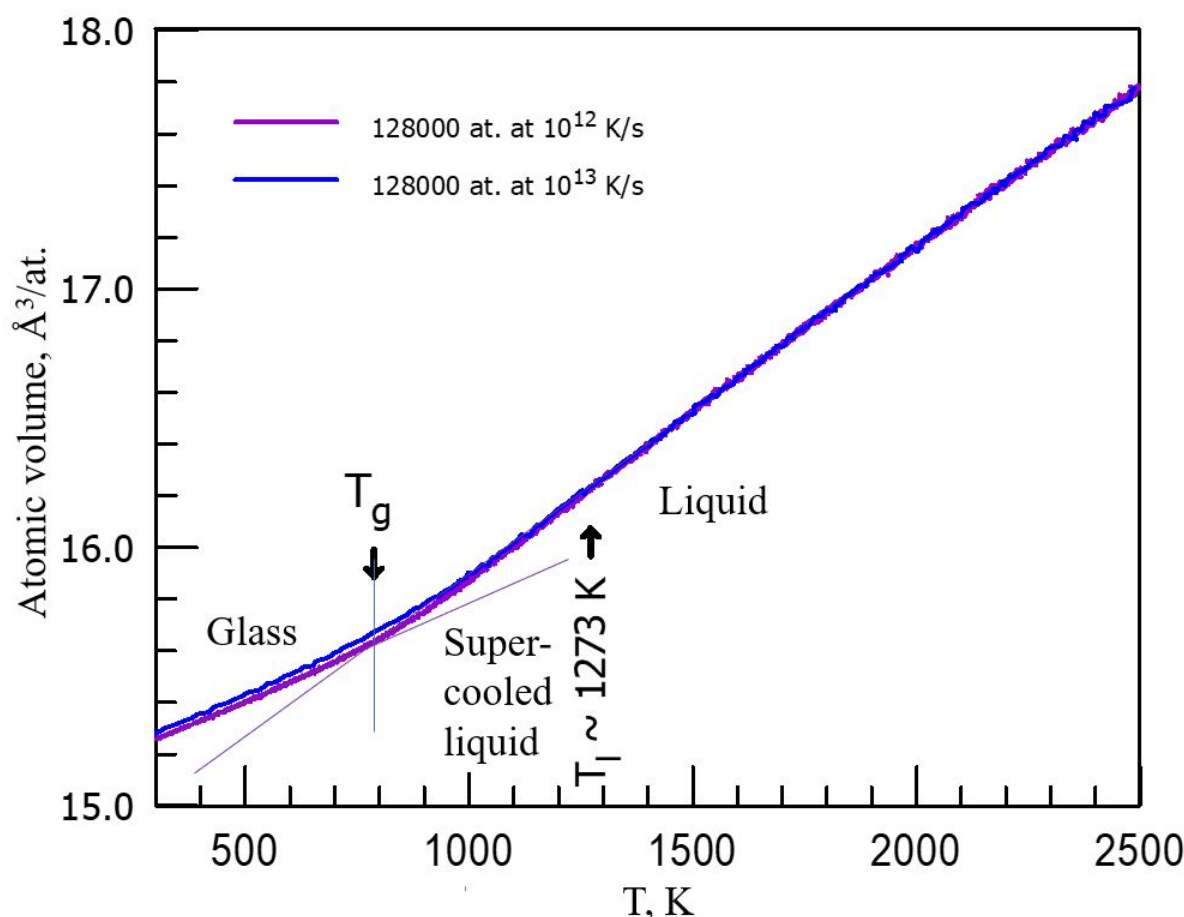


Fig. 3. Atomic volume of the simulated Ti_2Ni cells as function of temperature. There is a clear change in the slope at T_g and also a slight variation (with opposite sign) in the derivative dV/dT above T_l .

A change in the character of PDF_{\min} (Fig. 2) and atomic volume (Fig. 3) curves near the liquidus temperature (about 1273 K from the phase diagram) is rather related to the fragility of this liquid when it starts to reorganize its atomic structure on undercooling in the supercooled liquid (SCL) state (below T_l). Earlier structural changes in the liquid related to its fragility were observed in Pd-Cu-Ni-P alloy⁴⁷ and⁴⁸. The glass transition temperature of about 800 K obtained from both PDF_{\min} (Fig. 2) and atomic volume (Fig. 3) curves as a change of the slope. The intersection point of two fitting lines was found by segmented fitting and Akaike criterion⁴⁹ for segmented regression⁵⁰. It corresponds quite well to the experimental value of ~ 700 K obtained for Ti_2Ni alloy on heating⁵¹. It is about 100 K higher owing to very high cooling rate used at molecular dynamics simulation. It is worth noting again that the cooling rate used was $10^{12} - 10^{13}$ K/s. Namely that resulted in a considerable increase of the fictive T_g by ~ 100 K, which is expected accounting for known data on logarithmic dependence effects of cooling rate, see e.g.^{2, 52, 53}.

Connection of PDF features with configuron formation

Diffraction patterns are caused by neutron or X-ray diffraction on atoms therefore the values of PDF_{\max} and PDF_{\min} are proportional to the number of atoms that are positioned at average distances R_{\max} and R_{\min} correspondingly e.g. the higher PDF_{\max} and PDF_{\min} probabilities to

find atoms at these distances. Indeed, from equation (6) it follows that the average number of atoms in a shell of radius R with thickness $\delta \ll R$ is

$$n_{av} = 4\pi\rho_0 \int_{R-\delta/2}^{R+\delta/2} g(r)r^2 dr \cong 4\pi\rho_0 g(R)R^2\delta \quad (8)$$

Therefore, the average numbers of atoms N_{max} and N_{min} in the shells of radii R_{max} and R_{min} with thickness $\delta \ll R_{min}$ are:

$$N_{max} = 4\pi\rho_0 PDF_{max} R_{max}^2 \delta \quad (9a)$$

$$N_{min} = 4\pi\rho_0 PDF_{min} R_{min}^2 \delta \quad (9b)$$

where $PDF_{max} = g(R_{max})$ and $PDF_{min} = g(R_{min})$

From (9b) it follows that values of PDF_{min} are directly related to N_{min} e.g. shifts of atoms from the first coordination sphere. Such shifts of atoms occur due to bond-breaking processes and these can be caused by temperature fluctuations (pressure, irradiation) which is schematically shown in Fig. 4 for a SiO_2 glass.

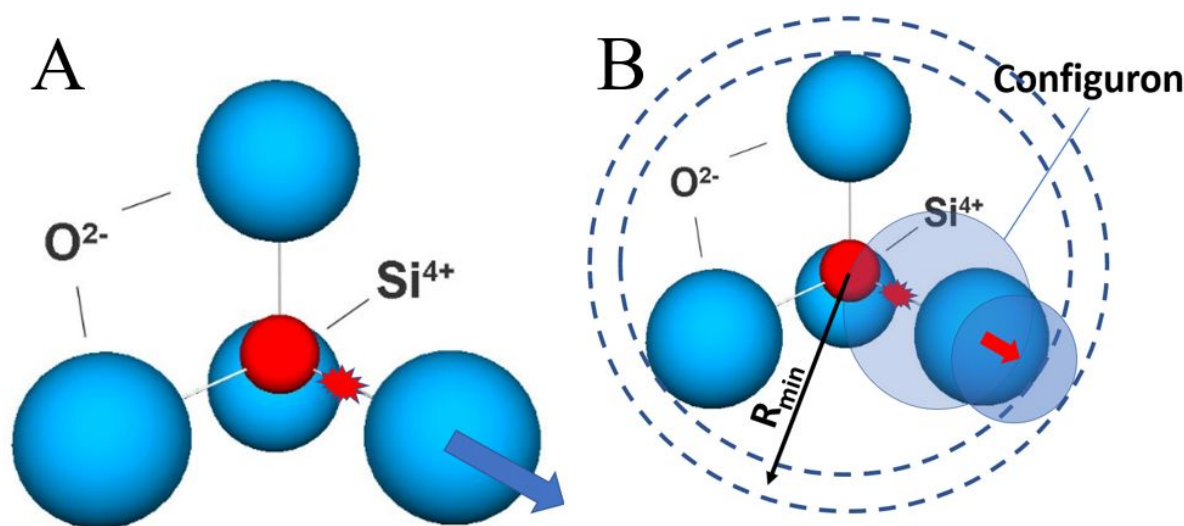


Fig. 4. (A) Bond breaking (shown as a red spot between Si^{+4} and O^{2-}) results in redistribution of oxygen atoms around silicon with an effective displacement (shift) of the oxygen out of first coordination shell. (B) Configuron is a broken bond with relaxed surroundings^{9, 25} and causes atomic displacements (shifts) that contribute to increase of FSDM of PDF.

A configuron is an elementary configurational excitation in an amorphous material, formed by breaking of a chemical bond (or transformation of an atom from one to another atomic shell) and the associated strain-releasing local adjustment of centres of atomic vibration^{9, 25}. The concept of configurons was not much exploited for amorphous metallic systems although namely local configurational excitations in the atomic connectivity network were shown to be the elementary excitations in high temperature metallic liquids and the bond-breaking mechanism, which leads to formation of configurons, was suggested as the fundamental excitation in metallic melts⁵⁴.

Metallic glasses and liquids contain significant topological and chemical short and medium range ordered units that increases with the cooling of the liquid^{55, 56}. Even at high temperatures, atoms tend to form local clusters although they are transient. Atoms switch from one cluster to the other rapidly, causing the local coordination number to increase or decrease. At high temperature the time that it takes for a cluster to gain or lose an atom is so

small that structural changes in one cluster have no impact on processes in nearby clusters. As the temperature is lowered, however, these changes and processes become cooperative^{35, 56}.

It is of primary importance that bond breaking processes e.g. formation of configurons in metallic glasses do also cause atomic displacements similarly to what happens in amorphous oxides. This is schematically shown in Fig. 5 for a conventional metallic glass using the example of Ni glass. It reveals that as a result of bond breaking process a Ni atom is released from the cluster containing a certain number of atoms. Schematically the empty space formed is considered as the configuron similarly to that happens in covalently bonded oxide glasses (Fig. 4).

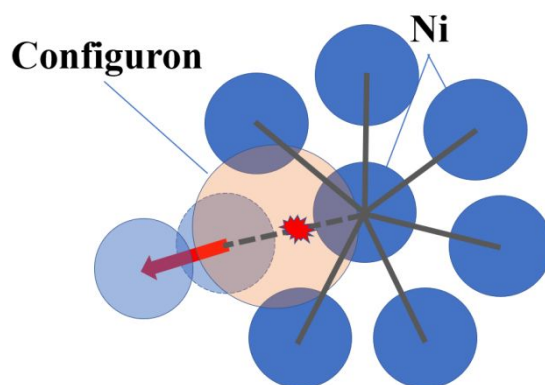


Fig. 5. Configuron formation in amorphous Ni due to change of the local atomic connectivity by losing or gaining one nearest neighbour following Egami et.al. concept⁵⁴.

The process schematically shown in Fig. 5 can readily occur when the bond is broken, and if enough free volume is available to accommodate the Ni atom released from the cluster of Ni atoms. More degrees of freedom and free accessible volume for atoms become available at higher temperatures in liquids when so many bonds are broken that they form macroscopic structures rather than point-like defects in glasses. Therefore, processes schematically shown in Fig. 5 are facilitated at temperatures exceeding T_g .

The crucial question is how to experimentally detect configurons which are elementary excitations rather than material entities? The way to do this is to detect some directly related consequences of configuron formation e.g. atomic displacements that can be revealed via neutron or X-ray diffraction. Indeed, temperature causes in amorphous materials bond breaking processes¹² correspondingly at higher temperature more configurons are formed and thus more atoms are displaced out of the first coordination shell e.g. they are shifted to distances corresponding to radii R_{min} . The higher temperature the higher $p(R_{min})$ which is proportional to PDF_{min} . However, on approaching and exceeding T_g the temperature behaviour of PDF_{min} will change. The reason of that change is that in the liquid state the topological organisation of bonds (geometry of bonds) drastically changes from 3D to a fractal geometry^{7, 8}.

Finding T_g from pair distribution function

Near T_g the relative content of configurons $\phi(T) = C_d/C_0$ can be linearized so that the equation will hold

$$\phi(T) = a + \text{tg}\alpha \cdot T \quad (10)$$

It should be accounted however that above the T_g the temperature proportionality coefficient $tg\alpha$ will change because a part of configurons will belong to the percolation cluster made of configurons and thus just a part of them will contribute to atomic displacements from initial positions in the CBL. We suggest therefore to analyse behaviour of PDF_{min} as a function temperature identifying the temperature where the $PDF_{min}(T)$ dependence exhibits a kink and allocate that temperature to glass transition temperature. We demonstrate that below in Fig. 6 for amorphous Ni where FSDM is given by upper $PDF_{min}(T)$ lines with experimental data taken from⁵⁷. The results of this work and an earlier one⁵⁸ using ab-initio modelling indicate T_g obtained at very high cooling rate when equilibrium liquid viscosity cannot be reached. The temperature for T_g in Ref.⁵⁷ is somewhat lower than that in Ref.⁵⁸ because of classical interatomic potential used in the former work. Ref.⁵⁸ gives more correct temperature. However, as the temperature dependence of density of liquid Ni (and volume) is nearly linear the isochoric (equivolume) glass transition temperature should be very close to that. It follows from the highest possible atomic number density of FCC lattice (the same as for HCP) compared to any other packing⁵⁹.

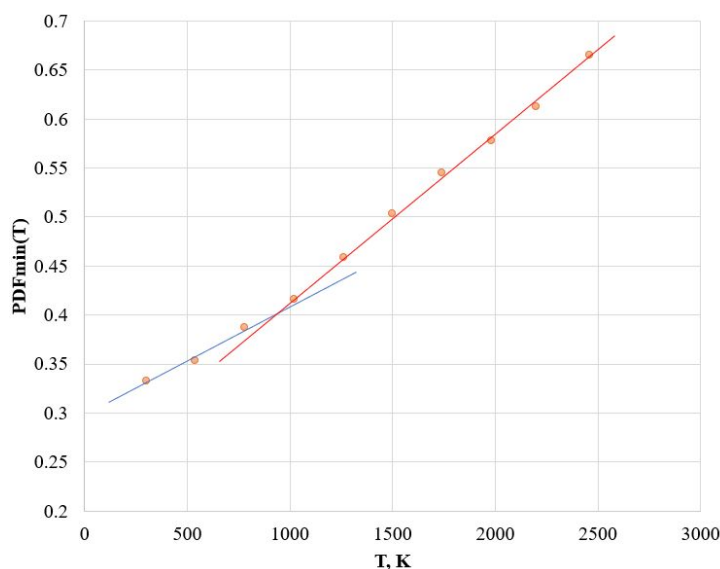


Fig. 6. Temperature dependences of first sharp diffraction minimum $PDF_{min}(T)$ for amorphous Ni: T_g is ~ 930 K⁵⁷.

We note that although assessing calculations based on Ref.⁶⁰ give a lower $T_g = 0.3777 \times T_m = 653$ K, Ni cannot have a so small T_g because the volume of such a glass would be much smaller than that of FCC crystalline Ni. It is known that T_g changes insignificantly in metallic alloys as a function of composition⁶¹. The reason why Ni has a relatively higher T_g is not because it is a good glass former. Molten Ni it is a very fragile liquid with fragility parameter D (from VFT equation) of only about 2⁶². Fragile liquids should be rather poor glass-formers⁶³. Thus, there is no contradiction between its high T_g and low glass-forming ability (GFA).

Finding the T_g using $PDF(T)$ dependences is not a new procedure: it was proposed as early as in 1972 by Wend and Abraham⁶⁴. However, the Wend and Abraham criterion is an empirical method without clearly understood processes behind it. We would like to briefly analyse below connection with it.

Connection with Wend-Abraham criterion

Wend and Abraham were the first who suggested to use the ratio $R_{WA}=PDF_{min}/PDF_{max}$ as a parameter describing a structural feature of the PDF, and who suggested as quantitative criterion for identifying the transition of amorphous phase from liquid to solid⁶⁴. Moreover, they first observed that the glass transition occurs at $R_{WA}=0.14$ and have proposed to use that as a “*criterion of the onset of the amorphous state by rapidly quenching and/or compressing a liquid*”. Wend and Abraham have suggested as possible hypothesis for explaining this feature the packing saturation of the first shell of nearest neighbour atoms.

We interpret that striking feature in terms of broken bond concept developed by Angel and Rao³⁰ and connect the experimentally found criterion $R_{WA}=0.14$ with condition of percolation in the system of broken bonds (in covalently or ionically bounded systems) termed configurons^{9, 25}. Indeed, the increase of temperature (also pressure or intensity of radiation^{12, 65}) causes in amorphous materials bond breaking correspondingly more atoms appear at borders of first coordination shell rather than within it and parameter $\phi(T)$ grows. The maximum value that parameter $\phi(T)$ can achieve is 1 and corresponds to a fully unbound system of atoms (gas) e.g. to a fully flattened PDF i.e. $g(r)$. Much earlier however dramatical changes occur in the topology of bonds of amorphous materials when parameter $\phi(T)$ will equal to universal Scher–Zallen critical density in the 3-D space $\theta_c=0.15\pm 0.01$ ^{28, 29} corresponding to percolation threshold in a system of broken bonds¹⁰ and the system of bonds of an amorphous material will change the geometry from a 3D to a fractal topology of dimensionality $D_f= 2.55\pm 0.05$ ⁷⁻¹⁴.

The fraction of broken bonds (configurons) $\phi(T)$ is a growing function of temperature and therefore is proportional to ratio N_{min}/N_{max} so that we can suppose that $\phi(T) = \frac{PDF_{min}}{PDF_{max}}$. We can hence assess the temperature of glass transition in amorphous materials using PDF data from equation

$$\phi(T_g) = \frac{PDF_{min}}{PDF_{max}} = \theta_c = 0.15 \pm 0.01 \quad (11)$$

As seen equation (11) practically reproduces the criterion introduced by Wendt and Abraham⁶⁴ who have found experimentally that PDF_{min}/PDF_{max} increases linearly with temperature changing the slope when $PDF_{min}/PDF_{max}=0.142$. Wendt and Abraham have first introduced the structural parameter designated here as R_{WA} which describes the structural feature of the PDF and then suggested as a quantitative criterion for identifying the amorphous phase change the $R_{WA}=0.14$. Following works have confirmed that all amorphous metallic systems studied exhibit this type of behaviour^{22-24, 57, 62}.

In practice, following Wendt and Abraham criterion, the T_g is found by approximating PDF_{min}/PDF_{max} (e.g. $\phi(T)$) by two lines and finding the intersection point of two fitting lines produced by segmented fitting. However, analysis of $PDF_{min}(T)$ instead of using Wendt and Abraham criterion is significantly more sensitive, apart that it has a clear physical sense behind. We demonstrate that below in Fig. 7 for amorphous Ni where FSDM is given by $PDF_{min}(T)$ lines.

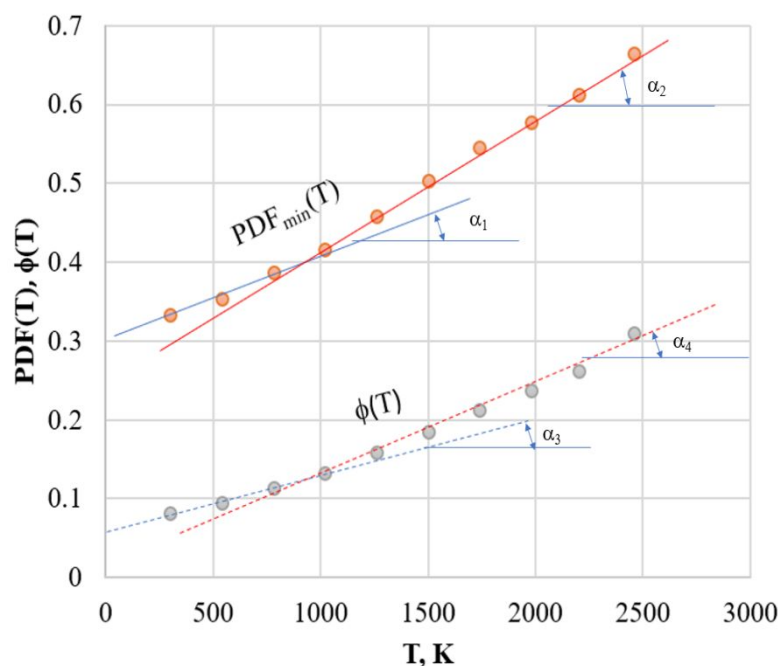


Fig. 7. Temperature dependences of $\text{PDF}_{\min}(T)$ and $\phi(T)$ for amorphous Ni.

As evident from Fig. 7 the kink in FSDM is almost twice sharper for $\text{PDF}_{\min}(T)$ than for $\phi(T)$ equivalent to Wendt and Abraham criterion which facilitates determination of T_g when analysing X-ray diffraction patterns. Indeed, for Ni we have $\text{tg}\alpha_2 / \text{tg}\alpha_1 \approx 2 \cdot \text{tg}\alpha_4 / \text{tg}\alpha_3$.

Discussion

We use in our theoretical treatment herewith the concept first proposed by Angell and Rao of configurons which are elementary excitations in the congruent bond lattice (CBL)²⁵. The bond model e.g. CBL provides straightforward answers if independent bonds are assumed⁶⁶. In this concept each broken bond plus associated strain-releasing adjustments of centres of atomic vibration is treated as an elementary configurational excitation termed configuron. Because local adjustments of centres of vibration requires some certain time there are unrelaxed configurons (instantaneously broken bonds) and relaxed configurons. Unrelaxed configuron are typical for computer simulations when the cooling rates are unrealistically high and cannot be achieved in experiments when both unrelaxed configurons are characteristic for highest cooling schedules and relaxed configurons occur for slower cooling rates.

The CBL is formed by chemical bonds and the configuron is thus associated with chemical bond concept which is readily linked to visualisation of bonds – see e.g. Fig. 4. Visualisation of chemical bonds is indeed an emerging topic in chemistry – see for example⁶⁷. By definition, a chemical bond is a lasting attraction between atoms, ions or molecules that enables the formation of chemical compounds. Chemical bonds are typically characterised as covalent, ionic and metallic. Fig. 4 illustrates the configuron formation in a system of covalent bonds, a similar figure can be readily drawn for ionic bonds as well. The case of metallic bonds could be considered at first glance somehow different. Indeed, metallic bonding is considered as resulting from collectivisation of outer shell electrons when each atom donates valence electrons to the so-called sea of almost free electrons which become associated with all atoms. However metallic bonding may be also considered as an extreme

example of delocalization of electrons over a large system of covalent bonds in which every atom participates. Metallic bonding is hence more collective in nature than ionic and covalent types. Atoms in metals are attracted to each other in a non-oriented way and this explains why metals are more easily deformed⁶⁷. Nevertheless, effectively the elementary act of gradual debonding on increase of temperature can be schematically considered as due to bond breaking although due to high mobility of excitations in metals it is difficult to exactly localise the configuron to a certain orientation. Notable that recent analysis of glasses relies as well on structural order parameters detecting sterically favoured structures in the instantaneous liquid states⁶⁸.

As bond breaking is inevitable associated by atomic displacements the direct consequence of that should be gradual change of coordination number (CN) with temperature for amorphous materials generically and metallic glasses and melts particularly. That kind of conclusions follow from the configuron percolation model of glass-liquid transition^{7-12, 69, 70}. Moreover, such kind of change of CN with temperature should be much more evident when the temperature exceeds T_g . It has been confirmed experimentally that CN gradually decreases with increase of temperature as shown in Fig. 8 below⁷¹.

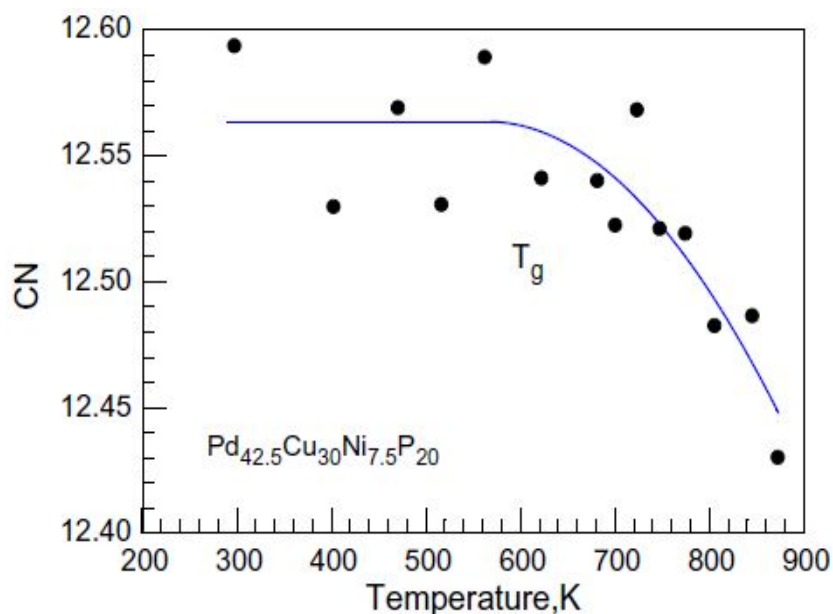


Fig. 8. Coordination number (CN) as a function of temperature for amorphous alloy $\text{Pd}_{42.5}\text{Cu}_{30}\text{Ni}_{7.5}\text{P}_{20}$ (Reproduced from⁷¹ with permission from Elsevier).

Data from Fig. 8 reveal that the CN changes much faster after T_g which conforms conclusions drawn from configuron percolation model of glass-liquid transition^{7-12, 69, 70}. However, temperature changes of CN cannot be used to identify T_g whereas data on behaviour of $\text{PDF}_{\min}(T)$ and $\phi(T)$ allow readily to identify T_g . Temperature behaviour of CN follows configuron percolation model predictions and is therefore supporting Wendt and Abraham approach to identification of temperature of glass transition.

Both Wendt and Abraham method, which is based on analysing $R_{\text{WA}}(T)=\phi(T)$, and the method proposed herewith, which is based on analysing $\text{PDF}_{\min}(T)$, can be used to identify T_g although the method based on FSDM is more sensitive. It is notable that the proposed method on analysing FSDM is related to main structural units of glasses which play the most important role in structural and dynamic features of metallic glasses^{22-24, 55, 57, 62, 68, 71}.

Conclusions

We proposed herewith to analyse temperature behaviour of FSDM (e.g. PDF_{min} as a function of temperature) identifying the temperature where the dependence exhibits a kink and allocate that temperature to glass transition temperature, T_g. The method proposed is more sensitive compared with empirical criterion of Wendt-Abraham e.g. for amorphous Ni the kink that determines T_g is almost twice sharper. A connection between Wendt-Abraham criterion and percolation via broken bonds (configurons) in amorphous materials is revealed.

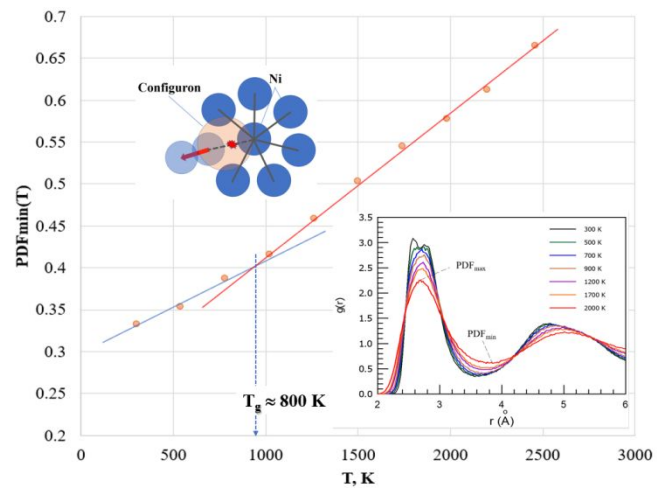
References

1. Angell, C. A.; Ngai, K. L.; McKenna, G. B.; McMillan, P. F.; Martin, S. W. Relaxation in Glassforming Liquids and Amorphous Solids. *Appl. Phys. Rev.* **2000**, *88*, 3113–3157.
2. Sanditov, D. S.; Ojovan, M. I. On Relaxation Nature of Glass Transition in Amorphous Materials. *Physica B*, **2017**, *523*, 96–113.
3. Tournier R. F. First-order Transitions in Glasses and Melts Induced by Solid Superclusters Nucleated and Melted by Homogeneous Nucleation Instead of Surface Melting, *Chem. Phys.* **2019**, *524*, 40-54.
4. *Encyclopedia of Glass Science, Technology, History, and Culture*. Richet P., Ed., Wiley, Hoboken, NJ, 2020.
5. Mazurin, O. V.; Gankin, Yu. V. Glass Transition Temperature: Problems of Measurement Procedures. *Glass Technology*, **2008**, *49*, 229-233.
6. *IUPAC. Compendium of Chemical Terminology*. Royal Society of Chemistry, Cambridge, 1997, Vol. 66, p. 583.
7. Ojovan, M. I.; Lee, W.E. Topologically Disordered Systems at the Glass Transition. *J. Phys.: Condensed Matter*, **2006**, *18*, 11507-11520.
8. Ozhovan, M. I. Topological Characteristics of Bonds in SiO₂ and GeO₂ Oxide Systems at Glass-liquid Transition. *J. Exp. Theor. Phys.*, **2006**, *103*, 819-829.
9. Ojovan, M. I. Configurons: Thermodynamic Parameters and Symmetry Changes at Glass Transition. *Entropy*, **2008**, *10*, 334-364.
10. Ojovan, M. I. Glass Formation in Amorphous SiO₂ as a Percolation Phase Transition in a System of Network Defects. *J. Exp. Theor. Phys. Lett.*, **2004**, *79*, 632-634.
11. Ojovan, M. I. Viscosity and Glass Transition in Amorphous Oxides, *Advances in Condensed Matter Physics*, **2008**, Article 817829.
12. Ojovan, M. I. Ordering and Structural Changes at the Glass-liquid Transition. *J. Non-Cryst. Solids*, **2013**, *382*, 79-86.
13. Stanzione III, J. F.; Strawhecker, K. E.; Wool R. P. Observing the Twinkling Nature of the Glass Transition, *J. Non-Cryst. Sol.*, **2011**, *357*, 311-319 .
14. Albert, S.; Bauer, Th.; Michl, M.; Biroli, G. ; Bouchaud, J.-P.; Loidl, A. ; Luckenheimer, P.; Tourbot, R. ; Wiertel-Gasquet, C.; Ladieu, F. Fifth-order Susceptibility Unveils Growth of Thermodynamic Amorphous Order in Glass-formers, *Science*, **2016**, *352*, 1308-1311.
15. Sanditov, D. S. Model of Delocalized Atoms in the Physics of the Vitreous State. *J. Exp. Theor. Phys.*, **2012**, *115*, 112-124.
16. Kirkpatrick, T. R. Mode Coupling Theory of the Glass Transition. *Phys. Rev. A*. **1985**, *31*, 939-944.
17. Kirkpatrick, T. R.; Thirumalai, D. ; Wolynes, P. G. Scaling Concepts of Viscous Liquids Near an Ideal Glassy State, *Phys. Rev. A.*, **1989**, *40*, 1045-1054.

18. *Encyclopedia of Polymer Blends: Volume 3: Structure, First Edition*. Edited by Avraam I. Isayev. Wiley-VCH, Weinheim, Germany 2016, pp 1-134.
19. Xia, X.; Wolynes P. G., Fragility of Liquids Predicted from the Random First-order Transition Theory of Glasses. *Proc. Natl. Acad. Sci. U.S.A.* **2000**, *97*, 2990-2994.
20. Tournier, R. F. Fragile-to-fragile Liquid Transition at T_g and Stable-glass Phase Nucleation Rate Maximum at the Kauzmann Temperature, *Physica B*, **2014**, *454*, 253-271.
21. Tournier, R. F. Glass Phase and Other Multiple Liquid-to-liquid Transitions Resulting from Two-liquid Competition, *Chem. Phys. Lett.*, **2016**, *665*, 64-70.
22. Oreshkin, A. I.; Mantsevich, V. N.; Savinov, S. V.; Oreshkin, S. I.; Panov, V. I.; Yavari, A. R.; Miracle, D. B.; Louzguine-Luzgin, D. V. In situ Visualization of Ni-Nb Bulk Metallic Glasses Phase Transition. *Acta Mater.* **2013**, *61*, 5216–5222.
23. Louzguine-Luzgin, D. V.; Chen, N.; Churymov, A. Y.; Battezzati, L.; Yavari, A. R. Role of Different Factors in the Glass-forming Ability of Binary Alloys. *J. Mater. Sci.* **2014**, *50*, 1783–1793.
24. Louzguine-Luzgin, D. V.; Seki, I.; Ketov, S. V.; Louzguina-Luzgina, L. V.; Polkin, V. I.; Chen, N.; Fecht, H.; Vasiliev, A. N.; Kawaji, H. Glass-transition Process in an Au-based Metallic Glass. *J. Non-Cryst. Solids*, **2015**, *419*, 12–15.
25. Angell, C. A.; Rao, K.J. Configurational Excitations in Condensed Matter, and the “Bond Lattice” Model for the Liquid-glass Transition. *J. Chem. Phys.*, **1972**, *57*, 470-481.
26. Suzuki, M.; Masaki, Y.; Katagawa, A. Model of the Glass Transition in Amorphous Solids Based on Fragmentation. *Phys. Rev. B*, **1996**, *53*, 3124-3131.
27. Torquato, S.; Stillinger, F. H. Jammed Hard-particle Packings: From Kepler to Bernal and Beyond. *Rev. Mod. Phys.*, **2010**, *82*, 2633–2672.
28. Isichenko, M. B. Percolation, Statistical Topography, and Transport in Random Media. *Rev. Mod. Phys.* **1992**, *64*, 961-1043.
29. Scher, H.; Zallen, R. Critical Density in Percolation Processes. *J. Chem. Phys.*, **1970**, *53*, 3759–3761.
30. Turnbull, D.; Cohen, M. H. On the Free-volume Model of the Liquid-glass Transition, *J. Chem. Phys.* **1970**, *52*, 3038-3041.
31. Tournier R. F. Homogeneous Nucleation of Phase Transformations in Supercooled Water. *Physica B*. **2020**, *579*, 411895.
32. Wei, S.; Yang, F.; Bednarcik, J.; Kaban, I.; Shuleshova, O.; Meyer, A.; Busch, R. Liquid-liquid Transition in a Strong Bulk Metallic Glass-forming Liquid. *Nature Commun.* **2013**, *4*, 2083.
33. Fischer, H. E.; Barnes, A. C.; Salmon, P. S. Neutron and X-ray Diffraction Studies of Liquids and Glasses. *Rep. Prog. Phys.* **2006**, *69*, 233–299.
34. Soper, A. K. The Radial Distribution Functions of Water as Derived from Radiation Total Scattering Experiments: Is There Anything We Can Say for Sure? *ISRN Physical Chemistry*, **2013**, 279463.
35. Egami, T.; Iwashita, T.; Dmowski, W. Mechanical Properties of Metallic Glasses. *Metals*, **2013**, *3*, 77-113.
36. Faber, T. E.; Ziman, J. M. A Theory of Electrical Properties of Liquid Metals 3. Resistivity of Binary Alloys, *Philosophical Magazine*, **1965**, *11*, 153-173.
37. Ma, D.; Stoica, A. D.; Wang, X.-L. Power-law Scaling and Fractal Nature of Medium-range Order in Metallic Glasses, *Nature Materials*, **2009**, *8*, 30-34.
38. Dinga, J.; Asta, M.; Ritchie, R. O. On the Question of Fractal Packing Structure in Metallic Glasses. *Proc. Natl. Acad. Sci. U.S.A.*, **2017**, *114*, 8458–8463.

- 1
2
3
4
5
6
7
8
9
10
11
12
13
14
15
16
17
18
19
20
21
22
23
24
25
26
27
28
29
30
31
32
33
34
35
36
37
38
39
40
41
42
43
44
45
46
47
48
49
50
51
52
53
54
55
56
57
58
59
60
39. Louzguine-Luzgin, D. V.; Georganakakis, K.; Tsarkov, A.; Solonin, A.; Honkimaki, V.; Hennes, L.; Yavari, A. R. Structural Changes in Liquid Fe and Fe–B Alloy on Cooling, *Journal of Molecular Liquids*, **2015**, *209*, 233–238.
40. Plimpton, S. J. Fast Parallel Algorithms for Short-range Molecular Dynamics, *J. Comp. Phys.*, **1995**, *117*, 1-19.
41. Kirova, E.; Pisarev, V. System Size Effect on Crystal Nuclei Morphology in Supercooled Metallic Melt, *Journal of Crystal Growth*, **2019**, *528*, 125266.
42. Wang, Z.; Chen, C. L.; Ketov, S. V.; Akagi, K.; Tsarkov, A. A.; Ikuhara, Y.; Louzguine-Luzgin, D. V. Local Chemical Ordering Within the Incubation Period as a Trigger for Nanocrystallization of a Highly Supercooled Ti-based Liquid, *Materials & Design*, **2018**, *156*, 504-513.
43. Nose, S. A Unified Formulation of the Constant Temperature Molecular Dynamics Methods, *Journal of Chemical Physics*, **1984**, *81*, 511-519.
44. Hoover, W. G. Canonical Dynamics, Equilibrium Phase-space Distributions, *Physical Review A*, **1985**, *31*, 1965-1967.
45. Berendsen, H. J. C.; Postma, J. P. M.; van Gunsteren, W. F.; DiNola, A.; Haak, J. R. Molecular Dynamics with Coupling to an External Bath *The Journal of Chemical Physics*, **1984**, *81*, 3684-3690.
46. Stukowski, A. Visualization and Analysis of Atomistic Simulation Data with OVITO - the Open Visualization Tool, *Modelling Simul. Mater. Sci. Eng.*, **2010**, *18*, 015012.
47. Louzguine-Luzgin, D. V.; Belosludov, R.; Yavari, A. R.; Georganakakis, K.; Vaughan, G.; Kawazoe, Y.; Egami, T.; Inoue, A. Structural Basis for Supercooled Liquid Fragility Established by Synchrotron-radiation Method and Computer Simulation, *Journal of Applied Physics*, **2011**, *110*, 043519.
48. Georganakakis, K.; Hennes, L.; Evangelakis, G. A.; Antonowicz, J.; Bokas, G. B.; Honkimaki, V.; Bytchkov, A.; Chen, M. W.; Yavari, A. R. Probing the Structure of a Liquid Metal During Vitrification, *Acta Materialia*, **2015**, *87*, 174-186.
49. Akaike, H. A New Look at the Statistical Model Identification, *IEEE Trans. Autom. Control*, **1974**, *19*, 716–723.
50. Muggeo, V. M. R. Interval Estimation for the Breakpoint in Segmented Regression: A Smoothed Score-based Approach, *Australian & New Zealand Journal of Statistics*, **2017**, *59*, 311–322.
51. Buchwitz, K. M.; Adlwarth-Dieball, R.; Ryder, P. L. Kinetics of the Crystallization of Amorphous Ti₂Ni, *Acta Metall. Mater.*, **1993**, *41*, 885-1892.
52. Li, F.; Zhang, H.; Liu, X.; Yu, C.; Lu, Z. Effects of Cooling Rate on the Atomic Structure of Cu₆₄Zr₃₆ Binary Metallic Glass. *Computational Materials Science*, **2018**, *141*, 59-67.
53. Buchholz, J.; Paul, W.; Varnik, F.; Binder, K. Cooling Rate Dependence of the Glass Transition Temperature of Polymer Melts: Molecular Dynamics Study. *J. Chem. Phys.*, **2002**, *117*, 7364-7372.
54. Iwashita, T.; Nicholson, D. M.; Egami, T. Elementary Excitations and Crossover Phenomenon in Liquids. *Phys. Rev. Lett.* **2013**, *110*, 205504.
55. Egami, T. Atomistic Theory of Metallic Liquids and Glasses. In: Miller M., Liaw P. (Eds) *Bulk Metallic Glasses*. Springer, Boston, MA, 2008.
56. Kelton, K.F. Kinetic and Structural Fragility—a Correlation Between Structures and Dynamics in Metallic Liquids and Glasses. *J. Phys.: Condens. Matter*, **2017**, *29*, 023002.

- 1
2
3
4
5
6
7
8
9
10
11
12
13
14
15
16
17
18
19
20
21
22
23
24
25
26
27
28
29
30
31
32
33
34
35
36
37
38
39
40
41
42
43
44
45
46
47
48
49
50
51
52
53
54
55
56
57
58
59
60
57. Louzguine-Luzgin, D. V.; Miyama, M.; Nishio, K.; Tsarkov, A. A.; Greer, A. L. Vitrification and Nanocrystallization of Pure Liquid Ni Studied Using Molecular-Dynamics Simulation *J. Chem. Phys.*, **2019**, *151*, 124502.
58. Louzguine-Luzgin, D. V.; Belosludov, R.; Saito, M.; Kawazoe, Y.; Inoue, A. Glass-transition Behavior of Ni: Calculation, Prediction, and Experiment, *Journal of Applied Physics*, **2008**, *104*, 123529.
59. Louzguine-Luzgin, D. V.; Inoue, A. An Extended Criterion for Estimation of Glass-forming Ability of Metals, *Journal of Materials Research*, **2007**, *22*, 1378-1383.
60. Tournier, R. F. Lindemann's Rule Applied to the Melting of Crystals and Ultra-stable Glasses. *Chem. Phys. Lett.*, **2016**, *651*, 198-202.
61. Li, Y. A Relationship Between Glass-forming Ability and Reduced Glass Transition Temperature Near Eutectic Composition, *Materials Transactions*, **2001**, *42*, 556 – 561.
62. Louzguine-Luzgin, D. V. Vitrification and Devitrification Processes in Metallic Glasses, *Journal of Alloys and Compounds*, **2014**, *586*, S2–S8.
63. Senkov, O. N. Correlation Between Fragility and Glass-forming Ability of Metallic Alloys. *Phys. Rev. B*, **2007**, *76*, 104202.
64. Wendt, H. H.; Abraham, F. F. Empirical Criterion for the Glass Transition Region Based on Monte Carlo Simulations. *Phys. Rev. Lett.* **1978**, *41*, 1244-1246.
65. Möbus, G.; Ojovan, M.; Cook, S.; Tsai, J.; Yang, G. Nano-scale Quasi-melting of Alkali-borosilicate Glasses Under Electron Irradiation. *J. Nucl. Mater.*, **2010**, *396* 264-271.
66. Angell, C. A.; Richards, B. E.; Velikov, V. Simple Glass-forming Liquids: their Definition, Fragilities, and Landscape Excitation Profiles. *J. Phys.: Condens. Matter*, **1999**, *11*, A75–A94.
67. Yashima, M.; Yonehara, Y.; Fujimori, H. Experimental Visualization of Chemical Bonding and Structural Disorder in Hydroxyapatite through Charge and Nuclear-Density Analysis. *The Journal of Physical Chemistry C*, **2011**, *115*, 25077-25087.
68. Tong, H.; Tanaka, H. Structural Order as a Genuine Control Parameter of Dynamics in Simple Glass Formers. *Nat. Commun.* **2020**, *10*, 5596.
69. Sanditov, D. S.; Ojovan, M. I. Relaxation Aspects of the Liquid-glass Transition. *Physics Uspekhi*, **2019**, *62*, 111 – 130.
70. Sanditov, D. S.; Ojovan, M. I.; Darmaev, M. V. Glass Transition Criterion and Plastic Deformation of Glass. *Physica B*, **2020**, *582*, 411914.
71. Georgarakis, K.; Louzguine-Luzgin, D.V.; Antonowicz, J.; Vaughan, G.; Yavari, A.R.; Egami, T.; Inoue, A. Variations in Atomic Structural Features of a Supercooled Pd–Ni–Cu–P Glass Forming Liquid During In Situ Vitrification. *Acta Materialia*, **2011**, *59*, 708–716.



TOC Figure